Disorder suppression and precise conductance quantization in constrictions of PbTe quantum wells

G. Grabecki,[1,*] J. Wróbel,[1] T. Dietl,[1,2,3] E. Janik,[1] M. Aleszkiewicz,[1] E. Papis,[4] E. Kamińska,[4] A. Piotrowska,[4] G. Springholz,[5] and G. Bauer[5]

[1]*Institute of Physics, Polish Academy of Science, al. Lotników 32/46, 02-668 Warszawa, Poland*

[2]*Institute of Theoretical Physics, Warsaw University, 00-681 Warszawa, Poland*

[3]*ERATO Semiconductor Spintronics Project, Japan Science and Technology Agency, al. Lotników 32/46, 02-668 Warszawa, Poland*

[4]*Institute of Electron Technology, al. Lotników 32/46, 02-668 Warszawa, Poland*

[5]*Institut für Halbleiter- und Festkörperphysik, Johannes Kepler Universität, A-4040 Linz, Austria*

(Received 29 June 2005; published 20 September 2005)

Conductance quantization was measured in submicron constrictions of PbTe, patterned into narrow 12 nm wide quantum wells deposited between $Pb_{0.92}Eu_{0.08}Te$ barriers. Because the quantum confinement imposed by the barriers is much stronger than the lateral one, the one-dimensional electron energy-level structure is very similar to that usually met in constrictions of AlGaAs/GaAs heterostructures. However, in contrast to any other system studied thus far, we observe precise conductance quantization in $2e^2/h$ units, *despite of a significant amount of charged defects in the vicinity of the constriction*. We show that such extraordinary results is a consequence of the paraelectric properties of PbTe, namely, the suppression of long-range tails of the Coulomb potentials due to the huge dielectric constant.

DOI: 10.1103/PhysRevB.72.125332 PACS number(s): 73.21.Hb, 72.80.Jc, 73.23.Ad, 77.22.Ch

I. INTRODUCTION

Present state-of-the-art epitaxial growth and processing techniques enable one to fabricate semiconductor nanostructures whose dimensions are comparable to the de Broglie wavelength of band carriers. Typical examples are narrow-point contacts whose conductance becomes quantized in $2e^2/h$ units,[1] as well as quantum dots revealing discrete energy levels, in close analogy to atomic levels.[2] Recently, much research effort has been devoted to quantum nanostructures because they could form the hardware basis of quantum information and communication technologies.[3,4] However, one of the problems to be solved prior to practical implementation is control over electrostatic potential on the nanometer scale.[5] Random potential fluctuations in nanostructures are produced either by unintentional defects introduced during the processing or heteroepitaxial growth or by artificially incorporated doping impurities. The latter cannot be completely avoided as they provide the free carriers necessary for the device operation. Modulation doping, in which the doped region is spatially separated from the free carriers, has been utilized as a means to elevate the problem and accordingly, up to now most of experimental results have been obtained for modulation doped AlGaAs/GaAs nanostructures.[6,7] However, even this almost perfect and developed system is not free of random potential fluctuations caused by the long-range tails of Coulomb potentials of the remote ionized dopants.[8,9]

The presence of potential fluctuations is responsible for the suppression of conductance quantization in modulation-doped wires longer than 0.5 μm, even though the electron mean-free path is longer than 10 μm.[10] This has stimulated the development of methods, such as carrier accumulation by means of external electrodes rather than by modulation doping.[11–14] Although this method allows one to observe conductance quantization in wires as long as 20 μm, at millikelvin temperatures they usually are obscured by irregular and reproducible fluctuations, indicating quantum interference of electron waves scattered by residual disorder. On the other hand, the enormous sensitivity of conductance quantization to even minute disorder can be used for the reciprocal purpose, namely, as a probe of nanoscale potential fluctuations. We exploit this here to demonstrate that the unique properties of PbTe[15] lead to an almost total suppression of the potential fluctuations, even in the presence of significant concentration of charged impurities and dislocations. We draw this conclusion from the observation of accurately quantized conductance steps in narrow constrictions lithographically patterned of PbTe/PbEuTe quantum wells, containing much more defects than AlGaAs/GaAs heterostructures. We assign this behavior to the paraelectric properties of PbTe, which result in a Curie-like temperature-dependent static dielectric constant, approaching a huge value of $\epsilon = 1350$ at 4.2 K.[16] Because the Coulomb potentials of charged defects are suppressed, the conducting electrons are only scattered by short-range potentials of defect and impurity cores, which makes the observation of ballistic transport phenomena possible. Thus, successful nanostructurization of this system would bring ideal quantum devices, free of the effects of nanoscale potential fluctuations.

Because of the lack of a perfect lattice-matched substrate and the resulting imperfections in PbTe epitaxial growth, there are some additional sources of disorder in the system. Although in our previous works we demonstrated the presence of conductance quantization in nanoconstrictions of wide, 50 nm thick PbTe quantum wells,[17–19] the perpendicular quantization energy was smaller than 1 meV and thus comparable to the lateral one. For this reason, one-dimensional (1D) energy levels were densely distributed and therefore even small potential fluctuations cause their over-

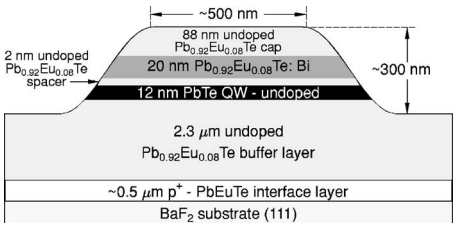

FIG. 1. Schematic view of the PbTe mesa cross section showing the layout of the initial layer grown by MBE.

lap. Additionally, because of the oval cross section of these constrictions, the higher 1D states were orbitally degenerate. Thus, although conductance steps were observed, they were neither flat nor did their magnitudes correspond exactly to the quantized values. Nevertheless, the small value of quantization energy together with the large magnitude of the Landé factor $|g^*| \approx 66$ made it possible to fabricate an efficient spin filter in which the spin-polarized current was transported by several waveguide modes, even in moderate magnetic fields of the order of only 1 T.[18] In the present work, we focus on submicron constrictions fabricated from much narrower PbTe quantum wells, where the two transverse quantization energies are significantly different. In these structures we demonstrate precise conductance quantization in $2e^2/h$ units despite significant charged defects in the vicinity of the constrictions. Thus, these nanostructures not only display a similar behavior as high-quality GaAs/AlGaAs wires, but also offer access to the region of lifted spin degeneracy of electron states already at low magnetic field.

II. MULTILAYER FABRICATION AND PROPERTIES

The multilayers used for fabrication of the constrictions were grown by molecular beam epitaxy (MBE) onto (111) BaF_2 substrate by using the protocols described, in detail, in Ref. 20. As shown schematically in Fig. 1, in the structures a 12 nm PbTe quantum well resides between $Pb_{0.92}Eu_{0.08}Te$ barriers. For this particular Eu composition, the barrier is as high as 235 meV. Because of the (111) growth direction, the fourfold *L*-valley degeneracy of the conduction band in PbTe is lifted, so that the ground-state two-dimensional (2D) subband is formed of a single valley with the long axis parallel to the [111] growth direction.[21] According to envelope function calculations,[21,22] the first excited subband is formed of the same valley and resides at ~24 meV above the ground state. The lowest state formed by the three remaining valleys, obliquely oriented to the growth directions, has a still higher energy of 35 meV above the ground state.

In order to introduce electrons into the quantum well, modulation doping by Bi ($N_D \approx 3 \cdot 10^{18}$ cm^{-3}) was employed with an undoped 2 nm wide $Pb_{0.92}Eu_{0.08}Te$ spacer layer separating the quantum well and the doping layer. This is much thinner than that usually employed in the case of the GaAs/AlGaAs system. Standard transport measurements reveal total electron density $n_{2D}=5.9\times10^{12}$ cm^{-2} and mobility 8.8×10^4 cm^2/Vs in the PbTe quantum wells at $T=4.2$ K. The analysis of Shubnikov–de Haas oscillations shows that at least five 2D subbands are occupied. The corresponding Fermi energy is evaluated to be at 80 ± 10 meV above the bottom of ground-state subband.

In the quantum well, the electron mobility is strongly reduced with respect to record values for the bulklike PbTe epilayers of up to 2×10^6 cm^2/Vs,[20] despite the application of the modulation doping. This results mainly from the strong alloy scattering[23] at the PbTe/$Pb_{0.92}Eu_{0.08}Te$ interfaces. Additionally, the system contains a significant number of threading dislocations formed during the initial growth on the BaF_2 surface due to 4.2% lattice mismatch. Most probably, they lead to formation of strongly *p*-type interface layer ($d \approx 0.4$ μm, $p > 10^{18}$ cm^{-3}) observed in transport measurements on PbTe layers of different thickness.[24] Such a *p*-type layer is also present in the case of $Pb_{0.92}Eu_{0.08}Te$ alloy.[19] Because the dislocation density is highest in the interface region, we can suppose that the dislocation-induced defects are electrically active and act as *p*-type doping. The application of a thick buffer layer reduces the dislocation density, which, however, remains still significant in the quantum-well region. This is shown by atomic force microscope (AFM) measurements performed on the as-grown $Pb_{0.92}Eu_{0.08}Te$ buffer layers where the dislocation density reaches 4×10^7 cm^{-2}. This is ~4 times larger than the value reported for pure PbTe epilayer of the same thickness.[25] Furthermore, the difference in thermal expansion coefficients between the whole layer structure and the BaF_2 substrate produces thermal strains of the order of 0.16% when the structure is cooled down to cryogenic temperatures.[20] There are experimental evidences that this strain induces movement of dislocations and produces additional defects.[26,27] Obviously, even a single of the enlisted mechanisms would preclude the observation of conductance quantization in a standard material. However, as we show below, this is not the case for PbTe because of its paraelectric nature.

III. FABRICATION AND PROPERTIES OF CONSTRICTIONS

PbTe nanostructures were fabricated by electron-beam lithography in the form of deeply etched mesas, employing the procedures described in our previous works.[17,19] A number of nanostructures of different forms was patterned. In the present work, we consider only two-probe conductance of constrictions, such as those marked by arrows in Fig. 2. Their width in the narrowest region is about 0.5 μm, and the total length about 1 μm. The insulating trenches have a depth of 0.3 μm. According to our previously established procedure,[19] an efficient tuning of the electron concentration in the constriction is possible by biasing the *p-n* junction that is formed between the p^+ interfacial layer and the *n*-type quantum well.

We have tested conductance of ten constrictions at 4.2 K. Six of them were conducting and tunable by the gate voltage. Two of this set have shown good conductance quantization, whereas for the others the quantization steps were significantly distorted. A possible origin is the presence of threading dislocations in the quantum-well region. Dislocation cores act not only as acceptors but produce also long-range

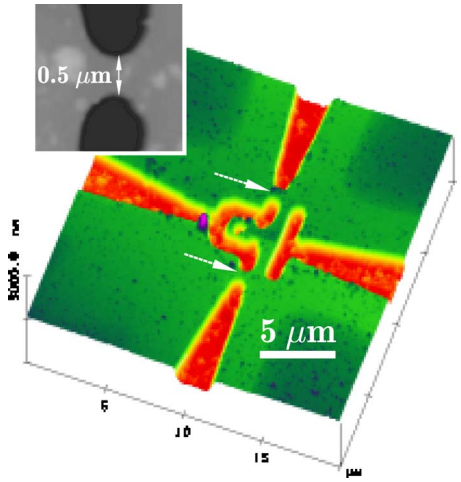

FIG. 2. (Color online) AFM image of a PbTe nanostructure. The studied constrictions are marked by arrows. Inset shows magnification of the constriction profile.

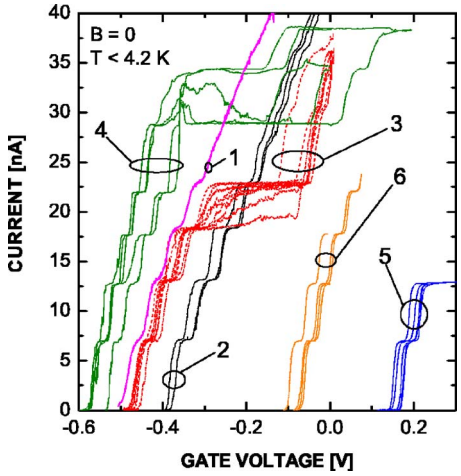

FIG. 3. (Color online) Experimental traces of the device current as a function of the gate voltage at zero magnetic field and at pumping helium temperatures. Particular sets of curves indicated by numbers have been obtained during subsequent measurement sessions.

strain fields vanishing as $1/r$.[28] Although the long-range Coulomb potential is expected to be suppressed by the lattice polarizability, the strain field remains largely unaltered and causes electron scattering. Therefore, the good structures are presumably those where the active region does not contain any dislocation. According to the AFM measurements of the dislocation density, the mean distance between dislocations is around 1.6 μm in our samples.

We have also found that electron motion in such structures is ballistic over the length scales at least 1 μm. We have observed classical ballistic effects in 1.6 μm wide Hall crosses prepared in the same way as the constrictions. In particular, we have found a large negative magnetoresistance dip occurring in weak magnetic fields below 50 K.[19,29] This is an indication of ballistic transmission of the electrons between opposite contact probes.

IV. CONDUCTANCE QUANTIZATION

Measurements of conductance quantization were performed by using the standard lock-in technique. An ac voltage of typical frequency of 129 Hz was applied to the large contact areas and the resulting current was measured. The voltage amplitude has been kept low enough to maintain the linear response. In Fig. 3, we show unprocessed experimental curves representing the device current as a function of gate voltage V_g in the absence of a magnetic field at 2 K. Individual curve sets were obtained during separate measurement sessions carried out in the course of nine months since device fabrication. Although there are large and nonmonotonic shifts of the threshold voltages in subsequent measurements, all curves show a series of regular steps at the same current values. For V_g exceeding +0.2 V, the gated p-n junction starts to conduct, precluding meaningful measurements. Interestingly, despite the rather high electron concentration in the unprocessed quantum well, a complete 1D channel depletion can be easily achieved in the narrow mesas. In some measurements, a full depletion occurs already at $V_g=0$ (Fig. 3, curve set No. 5), so that the application of a positive voltage is necessary to activate the channel. However, a significant depletion is observed only for constriction widths w of <0.5 μm. For wider constrictions, the conductance remains always high, for instance at $w=0.65$ μm, the conductance can be reduced only by about 20% even at $V_g=-0.9$ V, which is close to the gate breakdown limit. In certain cases (Fig. 3, curve sets No. 3 and 4), conductance hystereses are also observed when V_g is swept up and down. The set of results indicate that the number and positions of defects placed close to the constriction changes during thermal cycling and is also affected by the junction bias.

Conductance traces in $2e^2/h$ units obtained in various external magnetic fields B perpendicular to the surface during session No. 2 are summarized in Fig. 4. A series contact resistance of 140 Ω has been subtracted from the raw data. In the $B=0$ case, the four lowest conductance steps are equal to $i(2e^2/h)$; $(i=1,\ldots,4)$ with an accuracy better than 1%. Although further steps are less pronounced, one can easily resolve quantized conductance at values corresponding to $i=5$ 6, 8, and 10. It is well known that backscattering is sup-

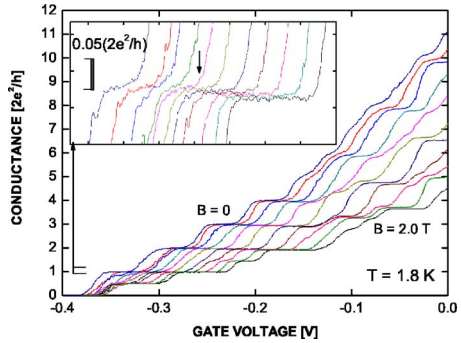

FIG. 4. (Color online) Constriction conductance as a function of V_g at 1.8 K in various magnetic fields from 0 to 2 T with a step 0.2 T. Inset shows magnification of the magnetic field evolution of the conductance step with the index $i=1$.

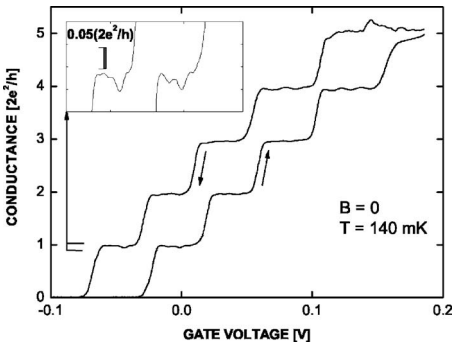

FIG. 5. Zero-field conductance as a function of V_g measured at millikelvin temperatures. Arrows denote directions of the voltage sweep. Inset shows magnification of one of the steps.

pressed by the magnetic field,[29] which should lead to an improvement of the step flatness. In the inset to Fig. 4, the step $i=1$ at various fields is shown on an enlarged scale. There is no visible improvement in the flatness up to 0.8 T (arrow), but in higher fields the step width starts to increase. At the same time a gradual decrease of the step height is observed, which arises from a contribution of the Hall effect in the macroscopic contact pads to the total device resistance. In higher magnetic fields, half-quantized steps start to develop, indicating the removal of spin degeneracy.

It is well known that scattering by random potentials leads to quantum interference,[30,31] which shows up as reproducible aperiodic conductance fluctuations that perturb the quantized step structure below 1 K.[32,33] Such low-temperature aperiodic fluctuations are even visible for constrictions of ultrapure GaAs/AlGaAs heterostructures with mobilities as high as 10^7 cm^2/Vs.[12] For this reason, we have examined our point contacts at millikelvin temperatures in order to probe of the effect of potential fluctuations upon the device characteristics. The measurements were carried out by using a ^{3}He/^{4}He dilution refrigerator, just before the measurement session No. 5 (see Fig. 3). As shown in Fig. 5, at 140 mK the conductance steps are even much sharper and flatter than those observed at 1.8 K. The inset shows magnification of the first conductance step, which reveals reproducible conductance fluctuations but with an amplitude of only a few percent of the total conductance.

V. DISCUSSION

The above findings clearly indicate that the confining potential of the electrons into 1D electron channels in PbTe is smooth at the scale of the constriction length of 1 μm. This seems to contradict the observation of the irreproducible shifts of the current traces shown in Fig. 3 that are obviously caused by changes in the defect distributions in the system. In order to resolve this problem, we have performed a simulation of the shape of the 1D confining potential of the constriction geometry shown in the inset to Fig. 2, taking into account the high dielectric constant of PbTe. In particular, we have calculated the potential at the narrowest part of the constriction, responsible for the conductance quantization. We have considered the near-depletion regime, where the

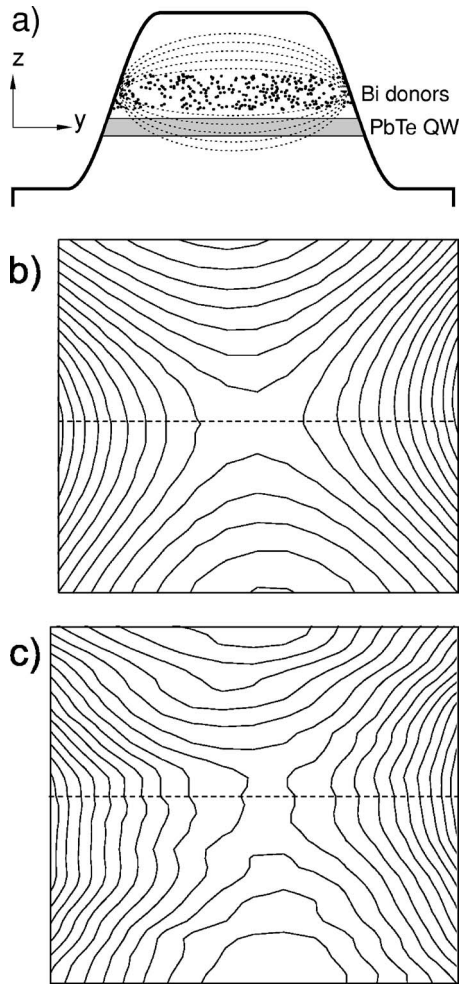

FIG. 6. (a) Schematic picture of the constriction cross section used for calculation of the 1D potential profile produced by randomly distributed donors (marked as black dots). Dotted lines indicate equipotential contours. (b) Calculated potential profile on the square of area 0.4×0.4 μm, in the x-y plane produced by uniformly distributed donor charge in the doping layer. Contours correspond to an energy spacing of 1 meV. (c) The same profile calculated for the charge of randomly distributed discrete donors.

contribution of the conducting electrons to the total potential can be neglected. This is justified because the background doping density, reaching 10^{17} cm^{-3},[20] is relatively high and just comparable to the estimated 1D electron density in the range where the lowest conductance steps are observed.[34] Then the 1D confining potential is entirely produced by positively charged donors randomly distributed in the doped layer, as it is illustrated schematically in Fig. 6(a).

Assuming a donor density of 3×10^{18} cm^{-3}, we have calculated the potential map in the PbTe quantum well by numerical summation of their Coulomb potentials. As a reference point, we have calculated the potential map for continuously distributed donor charge shown in Fig. 6(b). It represents a well-defined saddle-point potential. The calculation performed for discrete donors also gives a saddle-point, but there are visible distortions of the potential contours [Fig. 6(c)]. However, these deviations do not exceed 1 meV. In particular, the transverse confining potential at the

narrowest cross section (dashed lines) is practically the same in the both cases. We find that it is nearly parabolic with curvature corresponding to the 1D energy-level spacing $\hbar\Omega = 2.5$ meV. Importantly, this value depends only on the width of the donor stripe located just above the saddle point. We have checked this by carrying out the same calculations but with additional distributions of charges. For example, we have assumed various randomly distributed surface charges, volume charge corresponding to the background doping or the nondepleted electron charge in the wider regions of the constriction. In all these cases, the potential curvature, and thus the 1D level spacing, are practically the same. Obviously, this remains valid if the additional charge density is smaller than the doping donor density or its distance from the channel is appropriately large. The only effect produced by the additional charge is a rigid shift of the whole 1D energy-level structure.

Our simulations appears to explain pertinent experimental features. In particular, the calculated magnitude of the potential fluctuations is comfortably smaller than the 1D level spacing. In fact, the presence of screening by conducting electrons in real channels will reduce the potential fluctuations even more. Furthermore, the persistence of conductance quantization despite disorder results from the robustness of the parabolic potential curvature to the presence of randomly distributed charged defects. Because their potentials contribute merely to a constant potential background, they cause only a shift of the threshold voltage without deteriorating the step structure. In particular, the observed initial depletion of the channel is presumably caused by a large concentration of negatively charged defects existing in the constriction vicinity and/or on the device surfaces. One of possible candidates are negatively charged acceptors generated by dislocations. The significant shifts of the threshold voltage between different cooling sessions indicate a dominant role of the thermal stress in the defect redistribution, in accordance with previous magnetotransport measurements of 2D PbTe quantum-well structures.[26] Furthermore, the presence of hystereses when V_g is swept up and down indicates that the defect distribution is affected by the gate electric field that is of the order of 10^3-10^4 V/cm.

As shown in Fig. 4, a near-perfect conductance quantization is observed only for the steps with quantum numbers smaller than 5. This is because these 1D levels have an energy below the first excited 2D subband in the initial quantum well. For $i>4$, intersubband mixing starts to appear and we return to the situation encountered in the oval PbTe constrictions, where 1D energy levels exhibit orbital degeneracies.[19] From our calculations, the fifth 1D quantum level is at an energy, $4.5\hbar\Omega = 11$ meV, a value about two times smaller in comparison to calculated energy of the first excited subband. However, it should be recalled that for the potential simulations we have taken the geometrical profile (Figs. 1 and 2) for the width of the donor layer. If, for any possible reason this layer is narrower, $\hbar\Omega$ will increase. For example, one could suspect the existence of some donor compensation at the wire edges.

Our investigations in magnetic fields confirm the lack of potential fluctuations because there is no quantization improvement due to suppression of backscattering by the field. However, because of the small in-plane effective electron mass $m^* = 0.02m_0$, the Landau splitting becomes larger than $\hbar\Omega$ already at $B = 0.5$ T. Then the magnetic quantization dominates over the 1D wire quantization, and this causes a substantial widening of the steps. Similarly to other 1D systems, the steps gradually evolve into a quantum Hall-effect plateaux[29] with increasing widths.

Finally, it is worth mentioning that although the long-range tails of the Coulomb potentials are strongly suppressed, the short-range cores of the scattering potentials remain effective. Since the MBE growth of PbTe results in background donor concentration of the order of $10^{16}-10^{17}$ cm^{-3}, there are about 10–100 short-range scattering centers within the channel. Our data show, however, that they do not destroy the conductance quantization. One can recall here a number of theoretical models describing the conductance of 1D constrictions containing short-range scattering centers, approximated by the Dirac δ function.[35–38] The common result of these models is the strong dependence of the conductance quantization steps on the sign of the scattering potentials. In particular, for repulsive centers, the steps are altered rather weakly. However, the presence of attractive scatterers is predicted to produce large resonance dips superimposed on the steps. This remains valid even when extending the theory to scattering centers of small, but nonzero, range.[38] Because we do not have any independent information on the sign of the short-range part of impurity potentials in PbTe, the problem of their possible residual influence on conductance quantization remains open.

VI. SUMMARY

In conclusion, we have observed *precise* zero-field conductance quantization in submicron constrictions of PbTe quantum wells embedded in $Pb_{1-x}Eu_xTe$ barriers, similar to GaAs/AlGaAs quantum wires. We find a robustness of the conductance quantization against charged defects in the constriction vicinity, in a stark contrast to any other known systems. This results from the stressing of nanoscale Coulomb potential fluctuations by the huge static dielectric constant of PbTe. As a consequence, charge defects do not scatter the carriers but only shift the threshold voltage. At the same time, we do not see conductance resonances expected for scattering by short-range potentials, which may indicate that either the corresponding scattering cross sections are too small or that their potential is repulsive. Our results demonstrate the suitability of PbTe nanostructures as promising system for quantum devices.

ACKNOWLEDGMENTS

This work was partly supported by a PBZ/KBN/044/P03/2001 Grant, ERATO Semiconductor Spintronics Project, as well as the Gesellschaft fuer Mikroelektronik and the Fonds zur Foerderung der wissenschafftlichen Forschung of Austria.

*Electronic address: grabec@ifpan.edu.pl

[1] B. J. van Wees, H. van Houten, C. W. J. Beenakker, J. G. Williamson, L. P. Kouwenhoven, D. van der Marel, and C. T. Foxon, Phys. Rev. Lett. **60**, 848 (1988); D. A. Wharam, T. J. Thornton, R. Newbury, M. Pepper, H. Ahmed, J. E. F. Frost, D. G. Hasko, D. C. Peacock, D. A. Ritchie, and G. A. C. Jones, J. Phys. C **21**, L209 (1988).

[2] S. Tarucha, D. G. Austing, T. Honda, R. J. van der Hage, and L. P. Kouwenhoven, Phys. Rev. Lett. **77**, 3613 (1996).

[3] D. Loss and D. P. DiVincenzo, Phys. Rev. A **57**, 120 (1998).

[4] R. Hanson, L. H. Willems van Beveren, I. T. Vink, J. M. Elzerman, W. J. M. Naber, F. H. L. Koppens, L. P. Kouwenhoven, and L. M. K. Vandersypen, Phys. Rev. Lett. **94**, 196802 (2005).

[5] See, e.g., B. E. Kane, Nature (London) **393**, 133 (1998); Y. M. Galperin, B. L. Altshuler, and D. V. Shantsev, cond-mat/0312490 (unpublished).

[6] S. M. Cronenwett, H. J. Lynch, D. Goldhaber-Gordon, L. P. Kouwenhoven, C. M. Marcus, K. Hirose, N. S. Wingreen, and V. Umansky, Phys. Rev. Lett. **88**, 226805 (2002).

[7] A. C. Graham, K. J. Thomas, M. Pepper, N. R. Cooper, M. Y. Simmons, and D. A. Ritchie, Phys. Rev. Lett. **91**, 136404 (2002).

[8] J. A. Nixon, J. H. Davies, and H. U. Baranger, Phys. Rev. B **43**, 12638 (1991).

[9] M. A. Topinka, B. J. LeRoy, R. M. Westervelt, S. E. J. Shaw, R. Fleischmann, E. J. Heller, K. D. Maranowski, and A. C. Gossard, Nature (London) **410**, 183 (2001).

[10] G. Timp, *Semiconductors and Semimetals*, edited by M. Reed (Academic Press, New York, 1992), Vol. 35.

[11] R. H. Harell, K. S. Pyshkin, M. Y. Simmons, D. A. Ritchie, C. J. B. Ford, G. A. C. Jones, and M. Pepper, Appl. Phys. Lett. **74**, 2328 (1999).

[12] B. E. Kane, G. R. Facer, A. S. Dzurak, N. E. Lumpkin, R. G. Clark, L. N. Pfeiffer, and K. W. West, Appl. Phys. Lett. **72**, 3506 (1998).

[13] O. A. Tkachenko, V. A. Tkachenko, D. G. Baksheyev, K. S. Pyshkin, R. H. Harell, E. H. Linfield, D. A. Ritchie, and C. J. B. Ford, J. Appl. Phys. **89**, 4993 (2001).

[14] A. Yacoby, H. L. Stormer, K. W. Baldwin, L. N. Pfeiffer, and K. W. West, Solid State Commun. **101**, 77 (1997).

[15] For review of PbTe properties, see J. I. Ravich, B. A. Efimova, and I. A. Smirnov, *Semiconducting Lead Compounds* (Plenum, New York, 1968); G. Nimtz and B. Schlicht, edited by G. Höhler, Springer Tracts in Modern Physics Vol. 98 (Springer-Verlag, Berlin, 1983), p. 1; *Lead Chalcogenides Physics and Applications*, edited by D. Khokhlov (Taylor & Francis, London, 2003).

[16] See, e.g., G. Bauer, W. Jantsch, and E. Bangert, in *Advances in Solid State Physics*, edited by P. Grosse (Vieweg, Wiesbaden, 1983), Vol. XXIII, p. 27.

[17] G. Grabecki, J. Wrobel, T. Dietl, K. Byczuk, E. Papis, E. Kaminska, A. Piotrowska, G. Springholz, M. Pinczolits, and G. Bauer, Phys. Rev. B **60**, R5133 (1999).

[18] G. Grabecki, J. Wrobel, T. Dietl, E. Papis, E. Kaminska, A. Piotrowska, G. Springholz, and G. Bauer, Physica E (Amsterdam) **13**, 649 (2002).

[19] G. Grabecki, J. Wrobel, T. Dietl, E. Papis, E. Kaminska, A. Piotrowska, A. Ratuszna, G. Springholtz, and G. Bauer, Physica E (Amsterdam) **20**, 236 (2004).

[20] G. Springholz, in *Lead Chalcogenides Physics and Applications*, edited by D. Khokhlov (Taylor & Francis, London 2003), p. 123.

[21] S. Yuan, G. Springholz, G. Bauer, and M. Kriechbaum, Phys. Rev. B **49**, 5476 (1994).

[22] E. Abramof, E. A. de Andradee Silva, S. O. Ferreira, P. Motisuke, P. H. O. Rappl, and A. Y. Ueta, Phys. Rev. B **63**, 085304 (2001).

[23] A. Prinz, G. Brunthaler, Y. Ueta, G. Springholz, G. Bauer, G. Grabecki, and T. Dietl, Phys. Rev. B **59**, 12983 (1999).

[24] B. Tranta and H. Clemens, in *New Developments in Semiconductor Physics*, Lecture Notes in Physics Vol. 301, edited by G. Ferenczi and F. Beleznay (Springer Verlag, Berlin, 1988), p. 281.

[25] G. Springholz, A. Y. Ueta, N. Frank, and G. Bauer, Appl. Phys. Lett. **69**, 2822 (1996).

[26] M. M. Olver, J. Z. Pastalan, S. E. Romaine, B. B. Goldberg, G. Springholz, G. Ihninger, and G. Bauer, Solid State Commun. **89**, 693 (1994).

[27] H. Zogg, S. Blunier, A. Fach, C. Maissen, P. Muller, S. Teodoropol, V. Meyer, G. Kostorz, A. Dommann, and T. Richmond, Phys. Rev. B **50**, 10801 (1994).

[28] D. Hull and D. J. Bacon, *Introduction to Dislocations* (Pergamon Press, New York, 1984).

[29] C. W. J. Beenakker and H. van Houten, *Solid State Physics*, edited by H. Ehrenreich and D. Turnbull (Academic, New York, 1991), Vol. 44, p. 1.

[30] B. L. Altshuler and B. I. Skhlovskii, Zh. Eksp. Teor. Fiz. **91**, 220 (1986) [Sov. Phys. JETP **64**, 127 (1986)].

[31] P. A. Lee, A. D. Stone, and H. Fukuyama, Phys. Rev. B **35**, 1039 (1987).

[32] B. J. van Wees, L. P. Kouwenhoven, E. M. M. Willems, C. J. P. M. Harmans, J. E. Mooij, H. van Houten, C. W. J. Beenakker, J. G. Williamson, and C. T. Foxon, Phys. Rev. B **43**, 12431 (1991).

[33] J. Wrobel, F. Kuchar, K. Ismail, K. Y. Lee, H. Nickel, and W. Schlapp, Surf. Sci. **263**, 261 (1992).

[34] H. Schaber and R. E. Doezema, Phys. Rev. B **20**, 5257 (1979).

[35] P. F. Bagwell, Phys. Rev. B **41**, 10354 (1990).

[36] E. Tekman and S. Ciraci, Phys. Rev. B **42**, 9098 (1990).

[37] D. Boese, M. Lischka, and L. E. Reichl, Phys. Rev. B **62**, 16933 (2000).

[38] V. Vargiamidis and H. M. Polatoglou, Phys. Rev. B **71**, 075301 (2005).